Synthesis and DNA cleavage of 2′-*O*-amino-linked metalloporphyrin–oligonucleotide conjugates

Igor Dubey,† Geneviève Pratviel and Bernard Meunier *

Laboratoire de Chimie de Coordination du CNRS, 205 route de Narbonne, 31077 Toulouse cedex 4, France

Received (in Cambridge, UK) 2nd June 2000, Accepted 31st July 2000
Published on the Web 31st August 2000

A new general method for an easy 2′-O-modification of nucleosides is reported. We describe the preparation of modified 19-mer oligonucleotides carrying an aminoalkyl linker at the 2′-position of cytidine residues and the covalent attachment of an artificial chemical nuclease, a manganese(III) tris(*N*-methylpyridinium-4-yl)porphyrin moiety, onto the functionalized linker. The positions of attachment of the manganese cationic porphyrin within the 19-mer vector sequence and the length of the tether were selected in order to have the DNA-cleaver entity close to an $(AT)_3$-sequence in the duplex region formed by the 19-mer oligonucleotide vector and a single-stranded DNA target. The cleavage pattern of the target DNA by these new metalloporphyrin–oligonucleotide conjugates was compared with that obtained with the 19-mer oligonucleotide conjugate carrying the metalloporphyrin at the 5′-end.

Introduction

Diaquamanganese(III) *meso*-tetrakis(*N*-methylpyridinium-4-yl)porphyrin (Mn-TMPyP) is an efficient chemical nuclease when associated to $KHSO_5$, an oxygen-atom donor.[1] The mechanism of DNA cleavage involves the formation of a high-valent metal-oxo species[2–4] able to hydroxylate CH bonds of deoxyribose units of DNA[2–5] or to abstract electrons from the guanine bases.[6,7] The reactivity of oxo-Mn-TMPyP (sugar *versus* guanine oxidation) depends on the sequence of the DNA target. Mn-TMPyP has a high affinity for the minor groove of AT-rich regions of double-stranded B-DNA. Within that site, the oxidized form of Mn-TMPyP, namely oxo-Mn-TMPyP, mediates direct DNA breaks which are located on the 3′-side of each sequence consisting of three consecutive AT base pairs or $(AT)_3$-site.[5] These direct single-strand breaks are due to C-5′ hydroxylation of the deoxyribose moiety of the adjacent nucleoside on the 3′-side of the $(AT)_3$-site. The resulting products are fragments of DNA ending with a 3′-phosphate and a 5′-aldehyde respectively. Further reduction of the 5′-aldehyde into a 5′-OH function by $NaBH_4$ transformed the products of the oxidative cleavage into products of DNA hydrolysis.[8] Thus the interaction of Mn-TMPyP with its high $(AT)_3$-affinity site can afford a way to mediate the 'pseudo-hydrolysis' of the adjacent phosphodiester bond. When no $(AT)_3$-site is available on the target B-DNA, as well as in single-stranded DNA, the reactivity of the activated metalloporphyrin is shifted towards the oxidation of the guanines.[6,7]

In order to target this metalloporphyrin-based DNA-cleaving agent onto a specific region of DNA, an Mn-tris(methylpyridiniumyl) motif (Fig. 1) was covalently attached to an oligonucleotide (ODN) as a vector. The first generation of metalloporphyrin–ODN conjugates consisted of compounds with the metalloporphyrin moiety attached at the 5′-end of the ODN vector.[9–13] When these manganese cationic porphyrin–ODN conjugates were annealed with a long single-stranded DNA, the single-stranded target was damaged over several bases in the vicinity of the metalloporphyrin location, *i.e.* at the junction between the single- and the double-stranded DNA. The DNA degradation was mainly due to guanine oxidation in the single-stranded region of the target DNA, together with direct breaks due to C-5′ hydroxylations of the sugar in the AT-rich regions located in the double-stranded region of the conjugate/target hybrid.[10,11]

A large number of redox-active metallocomplexes, including Fe-EDTA, Fe-porphyrins, Cu-phenanthroline, Fe-bleomycin, Mn-porphyrins, metal-chelating peptides, *etc*. have been attached to oligonucleotides to produce sequence-specific chemical nucleases.[14,15] Among them, the cationic manganese tris(methylpyridiniumyl) motif is one of the most efficient artificial nucleases when attached at the 5′-end of an ODN.[9–13] This efficiency was rationalized in terms of closer interaction between the cationic nuclease and DNA.[13] However, in all these different cases, the ODN vector allowed the targeting of a selected sequence within large single- or double-stranded DNA targets but the cleavage pattern of these redox metal-based nuclease–ODN conjugates usually diffused over several nucleotide residues.[16–19] This is due to the fact that these chemical nucleases attached onto the ODN vector did not possess any special affinity or any strong specific binding site within the target DNA. We addressed the question whether it would be possible to build a metalloporphyrin–ODN conjugate which would allow us to take advantage of the proper high affinity of the Mn-tris(methylpyridiniumyl) motif for an $(AT)_3$-site. A metalloporphyrin–ODN conjugate capable of directing the metalloporphyrin to a single $(AT)_3$-site within the target DNA sequence and capable of promoting 'pseudo-hydrolysis' within this $(AT)_3$-site would represent a truly artificial restriction nuclease. Such a conjugate would promote the cleavage of a single phosphodiester bond on a strand of DNA and the resulting DNA fragments could be processed further. To favor the fitting of the metalloporphyrin with its favorite $(AT)_3$-binding site, the metalloporphyrin residue must be directed towards the minor groove of the duplex formed by the vector and its complementary target sequence. This could be done *via* an attachment to an oligonucleotide at a position oriented into the minor groove, *i.e.* at one 2′-position of sugar residue. By considering the structure of B-DNA, the functionalization of oligonucleotides by incorporating 2′-modified nucleosides seems to be the most convenient approach to target a DNA cleaver within the minor groove. Furthermore, as the 2′-position of deoxyribose in the duplex is just in the middle of the minor groove, the

† Present address: Institute of Molecular Biology and Genetics, National Academy of Sciences, Kiev, Ukraine.

 DOI: 10.1039/b004431h

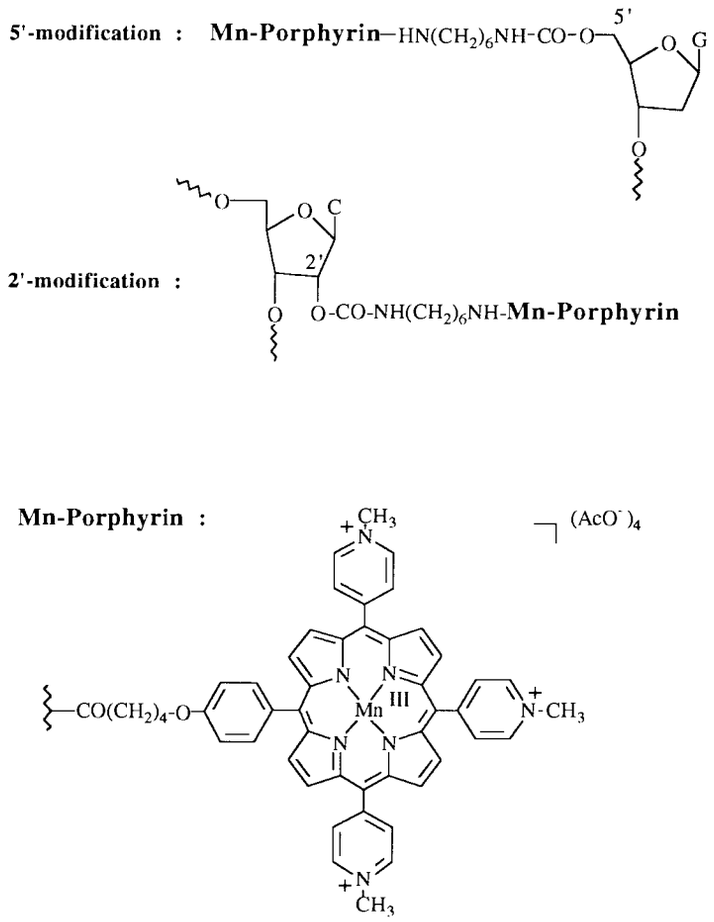

Fig. 1 Structures of the metalloporphyrin–oligonucleotide conjugates. The metalloporphyrin has two water molecules as axial ligands and thus an additional positive charge.

2′-linker groups should not sterically disturb formation of the duplex.

There are many reports on the preparation of 2′-O-modified nucleosides and oligonucleotides. The 2′-*O*-alkyl (especially methyl, as well as butyl, allyl, *etc.*) DNA analogs have been widely used in molecular biology.[20–22] Corresponding nucleosides are usually synthesized by alkylation of the 2′-hydroxy group of 3′,5′-protected nucleosides in the presence of sodium hydride. Oligonucleotides carrying at the 2′-position an intercalator group like anthraquinone,[23,24] anthracene[25] or pyrene[26] were obtained using 2′-O-modified nucleotide phosphoramidites. These latter derivatives were synthesized *via* alkylation of the 2′-hydroxy group of suitably protected nucleosides with the 2-(bromomethyl)anthraquinone, 2-(chloromethyl)-anthracene or 1-(chloromethyl)pyrene, respectively. As these alkylation reagents were benzyl halides, the alkylation reaction proceeded rather easily. Oligonucleotides having a dansyl fluorescence label at the 2′ position have been also synthesized. The key step in the preparation of the 2′-modified phosphoramidite was the reaction of 2′-amino-2′-deoxyuridine with dansyl chloride.[27] There are, however, only a few examples of a general method for introducing into oligonucleotides a 2′-linker suitable for the conjugation of a variety of different compounds. Manoharan *et al.* reported the synthesis of a 2′-*O*-(aminoalkyl)adenosine phosphoramidite. The synthetic method was based on the preferential 2′-O-alkylation (<5% of 3′-isomer) of non-protected adenosine with an alkyl halide in the presence of sodium hydride. Insertion of the corresponding phosphoramidite into oligonucleotides with subsequent deprotection yielded 2′-aminoalkylated oligomers which were then modified with fluorescein and other reporter groups.[28] A 2′-thiol tether was incorporated into oligonucleotides in a similar way, by 2′-O-alkylation of adenosine with *S*-protected 6-bromohexyl mercaptan in the presence of NaH, but the yield was only 27%.[29] Adenosine was also alkylated to prepare a series of common 2′-*O*-alkyl nucleoside derivatives for the incorporation into oligonucleotides.[30] However, selective alkylation reactions were only reported for non-protected adenosine. A more general way for the incorporation of a mercaptoalkyl linker into 2′-position of nucleosides was proposed by Douglas *et al.*[31] The multi-step synthesis was based on the alkylation of 3′,5′-*O*-silyl-protected nucleosides with ethyl bromoacetate in the presence of strong base with subsequent conversion of the 2′-*O*-substituent into a 2′-*O*-mercaptoethyl group. Nevertheless, O-alkylation of nucleosides is not a general and convenient approach, since a strong base like NaH must be used in the reaction, and is hardly compatible with several protecting groups.

In this report we propose a new general method for an easy 2′-O-modification of nucleosides. We describe the preparation of modified 19-mer-ODNs carrying an aminoalkyl linker at the 2′-position of cytidine residues and the covalent attachment of a metalloporphyrin moiety onto this functionalized linker. The site of conjugation of the manganese cationic porphyrin within the 19-mer vector sequence was selected taking into account the linker length so that the tethered nuclease residue would be close to an $(AT)_3$-site in the duplex region formed by the 19-mer-ODN vector and a single-stranded target. The cleavage of the target DNA by these new metalloporphyrin–ODN conjugates was compared with that of the 19-mer-ODN conjugate carrying the metalloporphyrin at the 5′-end.

Results and discussion

We assayed the DNA-cleavage activity of the metalloporphyrin–19-mer-oligonucleotide conjugates onto the single-stranded 35-

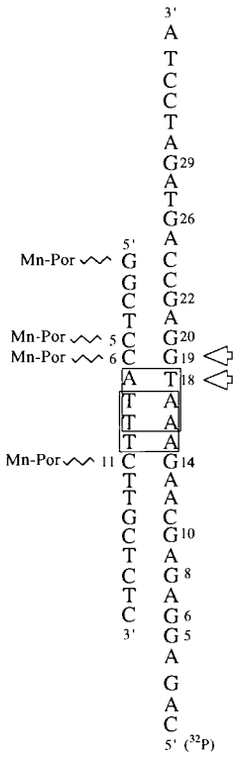

Fig. 2 Structure of the duplex formed by hybridization of the metalloporphyrin–19-mer ODN conjugates with the 35-mer single-stranded DNA target. The two $(AT)_3$-sites are shown by boxes. Mn-Por stands for the covalent attachment of a metalloporphyrin moiety. Each 19-mer vector is linked to one metalloporphyrin unit, but the four different possibilities of linkage are presented in this Figure. The arrows show the sites of cleavage of the 35-mer ODN by C-5′ hydroxylation of sugar. The 35-mer ODN was 5′-end-labelled.

mer-ODN, 5′-CAGAGGAGAGCAAGAAATGGAGCCAG-TAGATCCTA-3′ which is complementary to the 19-mer vector sequence from the G^6 to the C^{24} positions. The numbering of the nucleosides on ODNs starts at the 5′-side of the sequence. The oligonucleotide sequence of the 19-mer-ODN was thus 5′-GGCTCCATTTCTTGCTCTC-3′. The 2′-O-modified cytidines were positioned either at the C^5, C^6 or the C^{11} positions of the 19-mer-ODN. The resulting metalloporphyrin–ODN conjugates were C^5–Mn 19-mer, C^6–Mn 19-mer or C^{11}–Mn 19-mer, respectively (Figs. 1 and 2). These new metalloporphyrin-ODN conjugates were compared to the conjugate carrying the metalloporphyrin at the 5′-end of 19-mer ODN (Mn- 5′ 19-mer) (see also Figs. 1 and 2 for structure). The metalloporphyrin residue linked to the 2′-O-position of C^5 or C^6 in 19-mer-vector is forced to sit in the minor groove in the direction of the $(AT)_3$-site of the vector–target duplex. The metalloporphyrin tethered to the C-11 residue is oriented within the minor groove in the opposite direction with respect to the $(AT)_3$-sites.

Synthesis of modified phosphoramidite precursor

The synthesis of a cytidine phosphoramidite modified with 2′-aminoalkyl linker group (reagent **6**) is presented in Scheme 1. The 3′,5′-tetraisopropyldisiloxane (TPDS)-protected *N*-benzoylcytidine **1** was first treated with 1,1′-carbonyldiimidazole (CDI), affording nucleoside imidazolide **2**. It should be noted that starting nucleoside and product **2** have close R_f-values (0.81 and 0.77 in chloroform–methanol 9 : 1, respectively), and therefore the control of reaction by TLC was rather difficult; this was also the case for the transformation of **2** into **3**. Imidazolide **2** was purified by silica gel chromatography with a gradient of methanol (0–2.5%) in dichloromethane. Imidazolide **2** was treated with *N*-(trifluoroacetyl)hexamethylenediamine, prepared by monoacylation of hexamethylenediamine with ethyl trifluoroacetate. The nucleoside **3** bearing *N*-protected aminoalkyl linker was purified with the same gradient. Another possible way to transform **2** into **3**, by treating the imidazolide first with the diamine followed by protection of the end amino group with ethyl trifluoroacetate, was found to be less efficient, because of the formation of nucleoside dimer at the first step. The NMR spectrum of **3** clearly showed the disappearance of imidazole protons and the presence of NH and methylene group signals. The silyl protecting group was then removed by rapid treatment with tetrabutylammonium fluoride (TBAF) in tetrahydrofuran (THF), and 2′-O-modified cytidine derivative **4** was recrystallized from aq. ethanol. This nucleoside was 5′-O-tritylated by the standard method to give the protected nucleoside **5**. The latter was phosphitylated in dichloromethane. This reaction was relatively slow, because of the presence of the 2′-substituent, and was achieved in 1.5 h. Two diastereomers of the resulting phosphoramidite **6** were formed (total yield 74%) which could be separated by silica gel chromatography. The 'fast' isomer was eluted with $CHCl_3$–EtOAc–triethylamine (TEA) 7 : 2 : 1, whereas the 'slow' diastereomer was eluted with the same eluting system but in the proportions 45 : 45 : 10. Purity of diastereomers was >90% as was shown by ^{31}P NMR. The structure of all reaction products was confirmed by ^1H NMR spectroscopy and FAB-MS. The overall yield from cytidine was 22%. Although in the present work we have prepared only the 2′-modified cytidine reagent, this method is quite general and can be extended to other nucleosides.

Synthesis of manganese(III) tris(*N*-methylpyridinium-4-yl)-porphyrin–oligonucleotide conjugates

Cytidine carrying a 2′-*O*-aminoalkyl linker (**6**, Scheme 1) was then introduced in the sequence of the 19-mer ODN vector by phosphoramidite automated solid-phase synthesis. One modified cytidine residue was introduced in the sequence where it replaced a standard cytidine at position C^5, C^6 or C^{11} (see sequence of the 19-mer in Fig. 2). The coupling time for amidite reagent **6** (0.1 M in acetonitrile) was increased to 2 min. The coupling yield of 2′-modified amidite at C^5, C^6 and C^{11} positions was 95% when estimated by the trityl method (as in ref. 28) but appeared much lower, 65%, when calculated from the HPLC analysis of the crude product of the ODN synthesis. The lower yield of the coupling of the cytidine monomer carrying a 2′-*O*-aminoalkyl linker compared with that of an unmodified cytidine amidite was probably due to the steric effect of the 2′-*O*-alkyl substituent. The major impurity was an oligonucleotide corresponding to a stop at the nucleotide before the 2′-modified amidite (14-mer, 13-mer and 8-mer for the C^5-, C^6- and C^{11}-modified ODNs at retention times 33, 34 and 17 min, respectively, compared with 39 min for the full-length ODN). The trifluoroacetyl-blocked amine linker arm was fully deprotected during the ammonia cleavage and deblocking steps of oligonucleotide synthesis. The coupling of the metalloporphyrin moiety was performed as previously described [11,32] by formation of an amide bond between the activated ester of the metalloporphyrin and the alkylamine function of the various 2′-*O*-aminoalkyl ODNs. The Mn–C^5, Mn–C^6 and Mn–C^{11} 19-mer conjugates were obtained in very good yield (70%), with respect to the starting ODN, after HPLC purification on an anion-exchange column. The conjugated molecule with the metalloporphyrin at the 5′-end of the ODN sequence (Mn–5′ 19-mer) was included for comparison. The structures of the metalloporphyrin–ODN conjugates are shown in Fig. 1 and Fig. 2.

Cleavage of the 35-mer single-stranded DNA by the Mn–5′ 19-mer conjugate compared with that by the intra-strand, Mn–C^5, Mn–C^6 and Mn–C^{11} 19-mer conjugates

Comparative DNA-cleavage experiments were performed with the 5′-[^{32}P]labelled 35-mer-ODN at a final concentration of

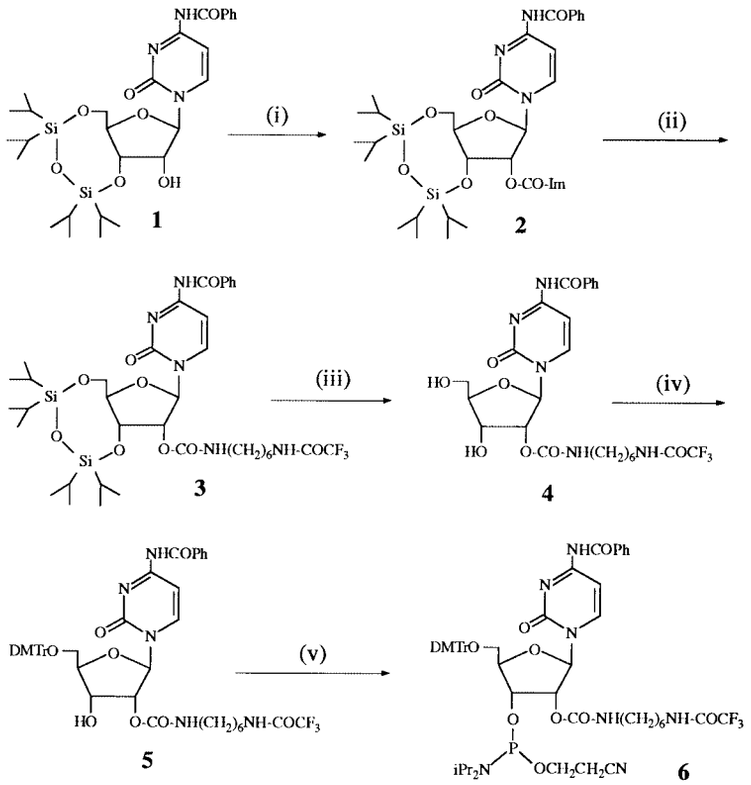

Scheme 1 Synthetic scheme for the preparation of 2′-O-modified phosphoramidite **6**. *Reagents, conditions and yields*: (i) CDI (1.5 eq.), CH_2Cl_2, 2 h (80%); (ii) $H_2N(CH_2)_6NHCOCF_3$ (2 eq.), CH_2Cl_2, 1.5 h (83%); (iii) TBAF (2.1 eq. in THF), 20 min (84%); (iv) DMTrCl (1.25 eq.), Py, 4 h (84%); (v) $Pr^i_2NP(Cl)OCH_2CH_2CN$ (2 eq.), DIPEA (4 eq.), CH_2Cl_2, 1.5 h (74%).

100 nM which was incubated with 100 nM of metalloporphyrin–oligonucleotide conjugates with an excess of random double-stranded herring testes DNA (0.2 mM base pairs) in 50 mM phosphate buffer (pH 7) and 100 mM NaCl. The results are reported in Fig. 3. The cleavage reaction was initiated by the addition of $KHSO_5$. After 1 h at 0 °C the reaction was stopped by the addition of an excess of HEPES‡ buffer which reacts with $KHSO_5$. The final concentration of $KHSO_5$ was 0.1 mM (Fig. 3, lanes 1–8) or 0.01 mM (Fig. 3, lanes 9–16). Direct DNA damage is illustrated through lanes 1–4 and lanes 9–12, with piperidine-labile breaks (shown as pip in Fig. 3) in lanes 5–8 and lanes 13–16 for 0.1 and 0.01 mM $KHSO_5$ concentrations, respectively. Each set of four lanes corresponded to the comparative analysis of the four different metalloporphyrin–ODN conjugates. The assays with the Mn–5′, Mn–C^5, Mn–C^6 and Mn–C^{11} 19-mer conjugates were loaded from left to right. The DNA fragments were identified according to the Maxam–Gilbert sequencing reaction (not shown). All these bands corresponded to the migration of 3′-phosphate-ending fragments.

In the presence of 0.1 mM of $KHSO_5$, extensive cleavage of the 35-mer target DNA by the Mn–5′ 19-mer conjugate consisted of a smear appearing in the G^{20}–G^{26} region of the sequence and two individual bands at G^{19} and T^{18} before piperidine treatment (Fig. 3, lane 1).[10,11] The G^{19} and T^{18} cleavage bands are due to the C-5′ hydroxylation of the G^{19} or T^{18} sugar residues for the metalloporphyrin interacting in the minor groove of the ($A^{16}A^{17}A^{18}$)-site and the ($A^{15}A^{16}T^{17}$)-site respectively. Extensive cleavage mediated by the Mn-5′ 19-mer conjugated molecule could be estimated by the very low intensity of the full-length material at the top of the gel (Fig. 3, lane 1). The smear was probably due to an altered mobility of the full-length DNA strand carrying multiple oxidative damage (several oxidized G's on the same strand under drastic oxidative conditions and probable partial lability of these lesions during electrophoresis). Upon piperidine treatment, the smear and a part of the full-length material were transformed into cleavage bands observed only at G residues (Fig. 3, lanes 5 and 13). At a low concentration of $KHSO_5$, lane 13 of Fig. 3, G^{26} was the main alkali-labile site. At higher concentrations of $KHSO_5$, lane 5, extensive oxidation of the 35-mer led to cleavage fragments mainly located at G^{19} residue. The labelled DNA probably included also some alkali-labile G-lesions located higher up on the gel and which were not visualized because only the shortest fragment with respect to the labelled 5′-end was observed in this case. The metalloporphyrin entity of the Mn–5′ 19-mer, attached onto the terminal G of the 19-mer vector, first reacted with the most accessible guanines in the single-stranded region of the 19-/35-mer duplex (G^{22}, G^{26}). Upon drastic oxidation conditions (0.1 mM $KHSO_5$, Fig. 3, lane 5), the activated metalloporphyrin was able to oxidize guanine bases in the double-stranded region or could reach also the $(AT)_3$-site where direct strand breaks were mediated by hydroxylation at C-5′ of the deoxyribose on the G^{19} and T^{18} residues. The reaction of the oxo-metalloporphyrin within the $(AT)_3$-sites occurred only after a significant degradation of the guanine bases, namely at a late stage of the reaction. This may be due to a partial dehybridization of the 19-/35-mer duplex in the region where guanines have been oxidized. The ratio of the reactivity of the oxo-metalloporphyrin towards G residues compared with one of the $(AT)_3$-sites was highly in favor of the oxidation at G bases.

In order to optimize the metalloporphyrin interaction in the minor groove of the $(AT)_3$-sites and to lower the G-oxidation, the metalloporphyrin entity was then positioned internally within the 19-mer sequence by its covalent attachment onto oligonucleotides containing a 2′-O-modified cytidine. The Mn–C^5 19-mer conjugate mediated direct cleavage at G^{19} and T^{18} (Fig. 3, lane 2) and alkali-labile lesion at the G^{19} residue (Fig. 3, lane 6). The difference in intensity of the G^{19} band in lane 6

‡ HEPES, 2-[*N*′-(2-hydroxyethyl)piperazin-*N*-yl]ethanesulfonic acid.

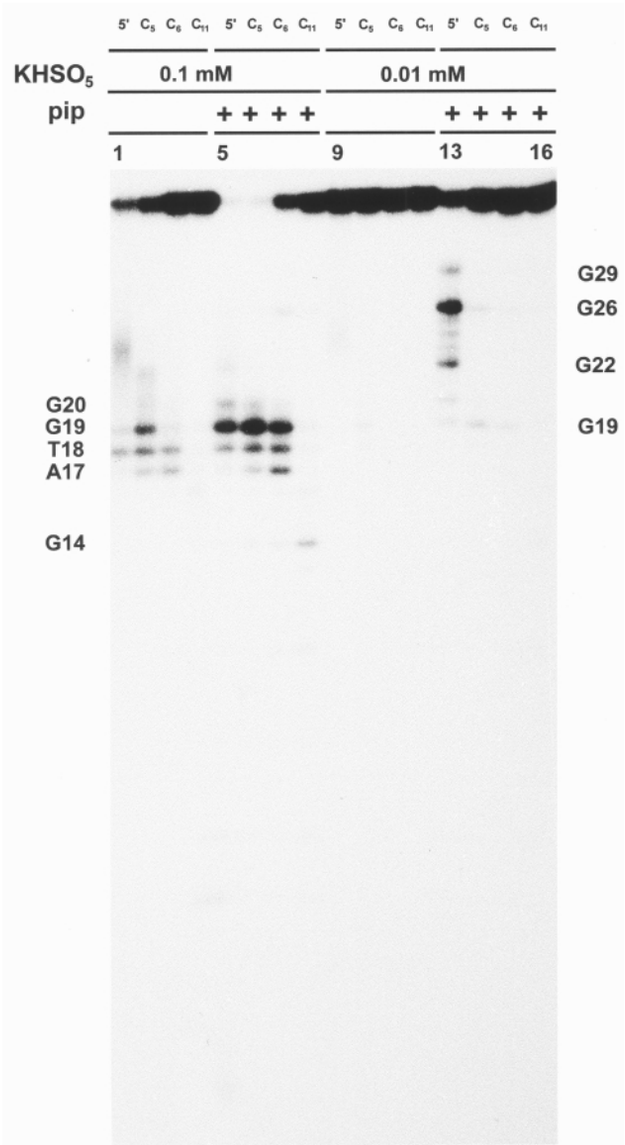

Fig. 3 Polyacrylamide gel analysis of the oxidative damage of the 5′-[^{32}P]labelled 35-mer ODN by the Mn–5′, Mn–C^5, Mn–C^6 and Mn–C^{11} 19-mer ODN conjugates in the presence of 0.1 (lanes 1 to 8) or 0.01 mM (lanes 9 to 16) of $KHSO_5$. The cleavage of the 35-mer target was monitored before (lanes 1 to 4 and 9 to 12) or after (lanes 5 to 8 and 13 to 16) piperidine treatment. Each set of four lanes corresponded to the comparative analysis of the four metalloporphyrin–ODN conjugates. The Mn–5′, Mn–C^5, Mn–C^6 and Mn–C^{11} 19-mer ODN conjugates assays were loaded from left to right. The bands of DNA fragments were identified according to the Maxam–Gilbert sequencing reaction. See Experimental for further details.

compared with that of lane 2 was indicative of the guanine oxidation mechanism *versus* the C-5′-hydroxylation mechanism on that residue. The metalloporphyrin covalently bound at C^5 of the 19-mer vector is now facing the G^{20} residue of the 35-mer target DNA (Fig. 2). One can note that the direct cleavage of the metalloporphyrin within the (A^{16}A^{17}T^{18})-site (G^{19}, direct cleavage) and the (A^{15}A^{16}A^{17})-site (T^{18}, direct cleavage) occurred at an earlier stage of DNA degradation indicating thus a better interaction of the C^5–Mn 19-mer metalloporphyrin moiety within the minor groove. After piperidine treatment (Fig. 3, lanes 5 and 6) these two conjugates showed the same pattern of cleavage but the internal metalloporphyrin (Mn–C^5 19-mer) probably mediated a more specific cleavage since comparison of lanes 13 and 14 of Fig. 3 clearly indicated that the intra-strand porphyrin did not react so well, at lower concentrations of $KHSO_5$, with the guanines of the single-stranded region of the target DNA, but probably only with G^{19}. The overall efficiency of the Mn–C^5 19-mer was lower than that of the terminal metalloporphyrin, as can be seen by comparison of the level of intact full-length material at the top of lanes 13 and 14 of Fig. 3 for the Mn-5′ and the Mn–C^5 19-mer conjugates, respectively.

The Mn–C^6 19-mer conjugate did not produce any smear before piperidine treatment and mediated direct breaks located downward on the gel, at T^{18} [(A^{15}A^{16}A^{17})-site] and A^{17} [(G^{14}A^{15}A^{16})-site] (Fig. 3, lane 3) at an even earlier stage of the reaction than with the C^5–Mn 19-mer ODN conjugate (compare the intensity of the full length DNA in lanes 2 and 3 or 6 and 7 in Fig. 3). The Mn–C^6 19-mer conjugate, as well as the Mn–C^5 19-mer one, showed that the metalloporphyrin reacted within the minor groove of the duplex DNA as a primary event of DNA degradation. No direct cleavage at the G^{19} residue was observed. The G^{19} band was only revealed as an alkali-labile site, indicating a guanine-oxidation mechanism (Fig. 3, lanes 3 and 7). In the case of the Mn–C^6 19-mer conjugate, no cleavage was observed in the single-stranded region (Fig. 3, lane 7). The metalloporphyrin now faced the G^{19} residue on the 35-mer sequence and was able to mediate oxidation of this guanine (whereas the previous Mn–C^5 19-mer conjugate did not oxidize the complementary G^{20} base). The efficiency of the Mn–C^6 19-mer was much lower than the two previously described conjugates. At 0.1 mM of $KHSO_5$ only 50% of the full length DNA was damaged after piperidine treatment (Fig. 3, lane 7) compared with a total degradation observed in lanes 5 and 6 of Fig. 3.

The Mn–C^{11} 19-mer conjugate did not find any $(AT)_3$-site to interact with since it was directed to the other side with respect to the AT-rich region of the duplex. The metalloporphyrin was facing the G^{14} residue on the target DNA. This compound allowed us to evaluate the reactivity of an internally located metalloporphyrin onto the guanine that is directly complementary to the modified cytidine residue. As shown in Fig. 3, lanes 4, 8 and lanes 12, 16, a weak oxidation of the G^{14} residue was evidenced only at high concentration of $KHSO_5$ (less than 10% of cleavage).

Concerning the direct cleavage within $(AT)_3$-sites by the metalloporphyrin conjugates tethered by 2′-linkers at different sites within the sequence of the 19-mer vector, the results can be summarized as follows. When the metalloporphyrin is attached in front of G^{20} (Mn–C^5 19-mer) direct damage at G^{19}, (A^{16}-A^{17}T^{18})-site, and T^{18}, (A^{15}A^{16}A^{17})-site, was observed, whereas when the metalloporphyrin was attached in front of G^{19} (Mn–C^6 19-mer) direct damage at T^{18}, (A^{15}A^{16}A^{17})-site, and A^{17}, (G^{14}A^{15}A^{16})-secondary site, was observed, no interaction with the upper box [G^{19} band for interaction within the (A^{15}A^{16}A^{17})-site] being possible. Thus the oxo-metalloporphyrin oxidized a CH-5′ bond of the nucleotide adjacent to the complementary base in the 5′-direction on the target DNA. The metalloporphyrin clearly interacted with the $(AT)_3$-site that is separated by one nucleotide unit in the direction on the 5′-end of the target sequence and this reactivity appeared as a primary event of DNA damage. However, the intra-strand tethered metalloporphyrins did not reach the high reactivity of the free metalloporphyrin, Mn-TMPyP, for the $(AT)_3$-sites.[5,8] With the 2′-linked metalloporphyrin conjugates, it has been possible to favor the approach of the metalloporphyrin entity to an $(AT)_3$-site, but without being able to tune the exact binding mode in order to hydroxylate one of the CH bonds at C-5′. These hydroxylation reactions are O-atom-transfer reactions and the high-valent metal-oxo species should approach very close to the H-atom that will be abstracted. Otherwise the oxo-manganese porphyrin behaves like a strong two-electron oxidant and abstracts electrons from the nearest guanine residues. This balance between CH-hydroxylation *versus* guanine oxidation is also dependent on the strength of the binding affinity of the cleaver within double-stranded DNA.

The reactivity towards guanine bases was found to account for the major mechanism of oxidative damage of the target DNA for the four tested metalloporphyrin–ODN conjugates. The guanines in a single-stranded region or belonging to a GG sequence in the double-stranded region of the vector/target hybrid were particularly reactive. The sensitivity of the guanines located in single-stranded regions was illustrated by the reaction of Mn–5′ 19-mer ODN conjugate at low concentrations of $KHSO_5$ (Fig. 3 lane 13), while the three other compounds were almost inactive under the same conditions. The easy GG oxidation was evidenced by the high efficiency of the Mn–C^5 19-mer conjugate (lane 6, Fig. 3). The accessibility of the G bases in the single-stranded region was probably responsible for the high efficiency of DNA degradation of 5′-end-modified conjugates (lane 13 of Fig. 3), and the low oxidation potential of a 5′-G of a GG sequence[33] explains the higher efficiency of the Mn–C^5 compared with the Mn–C^6 or Mn–C^{11} 19-mer conjugates. Concerning the intra-strand-located metalloporphyrins (Mn–C^5, Mn–C^6 and Mn–C^{11} 19-mer ODN conjugates), the Mn–C^6 derivative was able to oxidize the complementary paired G^{19} on the target DNA, while the Mn–C^{11} derivative reacted with the complementary G^{14} but to a much lower extent. The difference in oxidation of these two guanines may be explained by the higher oxidation potential of the isolated G^{14} compared with G^{19} (G^{19} is the 5′-G of a GG sequence).[33] The Mn–C^5 19-mer conjugate did not show any cleavage band corresponding to oxidation of the complementary G^{20} but exhibited the highest reactivity towards the G^{19} residue (one nucleoside shift in the 5′-direction of target). This result may be explained by a better positioning of the tethered metalloporphyrin towards a guanine shifted by one nucleotide unit (in the 5′-direction of the target DNA), as was observed in the case of the reaction within the $(AT)_3$-sites, due to the fact that the metalloporphyrin was forced to be oriented towards the 5′-direction of the target DNA. However, the total absence of G^{20} damage in the case of the Mn–C^5 19-mer conjugate might indicate the existence of transfer of oxidative damage from the G^{20} to the G^{19} base.[34–36]

Conclusions

The currently reported synthesis of a 2′-amino-linked cytidine allows site-selective positioning of a DNA cleaver and can be extended to the 2′-labelling of oligonucleotides with various molecules. The length and the chemical structure of linker can be selected to optimize interaction with the minor groove. The illustration of the variation in cleavage of DNA by different metalloporphyrin–oligonucleotide conjugates showed that the efficiency of the degradation of the target DNA, due to the binding of the 2′-linked-metalloporphyrin within the minor groove of $(AT)_3$-sites, was not significantly increased to favor the C-5′-hydroxylation of sugar units by the oxo-metalloporphyrin and to completely avoid neighbouring G-oxidation.

Experimental

General methods

Cytidine, 1,3-dichloro-1,1,3,3-tetraisopropyldisiloxane, CDI, 1,6-diaminohexane, TBAF, 4,4′-dimethoxytrityl chloride (DMTrCl), diisopropylethylamine (DIPEA), 2-cyanoethyl *N*,*N*-diisopropylchlorophosphoramidite, benzotriazol-1-yl-oxytris(dimethylamino)phosphonium hexafluorophosphate (BOP) and 1-hydroxybenzotriazole (HOBT) were purchased from Aldrich, ethyl trifluoroacetate from Lancaster. Anhydrous solvents were from Merck. Other commercially available reagents and all other solvents were purchased from standard chemical suppliers and used without further purification.

NMR spectra were recorded on a Bruker AM 250 spectrometer at 250 MHz for ^{1}H NMR or 101 MHz for ^{31}P NMR. External standards were tetramethylsilane and 85% H_3PO_4 for ^{1}H and ^{31}P NMR, respectively. Mass spectrometry analyses were performed on a Nermag R1010 apparatus [FAB^+/*m*-nitrobenzyl alcohol (MNBA) matrix] and a Perkin-Elmer SCIEX API 365 ESI-MS spectrometer (negative mode). TLC was performed on Alugram Sil G/UV_{254} plates (Macherey-Nagel) using $CHCl_3$–MeOH 9:1 (system A) and $CHCl_3$–EtOAc–TEA 45:45:10 (system B) as developers. The oligonucleotides were synthesized on an Expedite 8900 PerSeptive Biosystems instrument using commercially available reagents. Oligonucleotides were analyzed by HPLC using an anion-exchange column (Protein Pak DEAE 8 HR from Waters, 8 cm × 1 cm) eluted in a gradient mode (solvent A, 25 mM Tris/HCl, pH 8.5; solvent B, A + 1 M NaCl) from 20 to 40% of solvent B in 1 h, flow rate 0.7 ml min^{-1}. Detection was at 260 and/or 468 nm (diode array detector from Kontron).

Synthesis of modified phosphoramidite precursor 6

4-*N*-Benzoyl-3′,5′-*O*-(1,1,3,3-tetraisopropyldisiloxane-1,3-diyl)cytidine 1. Starting *N*-benzoylcytidine was prepared by the reaction of cytidine with benzoic anhydride in boiling ethanol (yield 91%), as per Watanabe and Fox.[37] It was silylated with 1,3-dichloro-1,1,3,3-tetraisopropyldisiloxane in pyridine to give **1** (yield 72%), as described previously.[38]

4-*N*-Benzoyl-2′-*O*-(imidazol-1-ylcarbonyl)-3′,5′-*O*-(tetraisopropyldisiloxane-1,3-diyl)cytidine 2. The 3′,5′-*O*-tetraisopropyldisiloxanediyl-*N*-benzoylcytidine **1** (783 mg, 1.33 mmol) was evaporated twice with anhydrous acetonitrile (2 × 15 ml), and dissolved in 10 ml of dry dichloromethane. CDI was added (1.5 eq., 2 mmol, 324 mg) and the reaction mixture was stirred at room temperature for 2 h. Mixture was directly applied to a silica column and product was isolated (gradient 0–2.5% MeOH in CH_2Cl_2). Corresponding fractions were evaporated under vacuum to give a white solid foam (726 mg, 80%); ^{1}H NMR ($CDCl_3$) δ 8.84 [br s, 1 H, NH (Cyt)], 8.22 (d, 1 H, H-6, $J_{6,5}$ 7.5 Hz), 8.16 (s, 1 H, imidazole), 7.89 (d, 2 H, Bz, *J* 7.1 Hz), 7.50–7.65 [m, 4 H, 3 H (Bz) + H-5], 7.44 (s, 1 H, imidazole), 7.09 (s, 1 H, imidazole), 6.06 (s, 1 H, H-1′), 5.63 (d, 1 H, H-2′, *J* 4.6 Hz), 4.48 (m, 1 H, H-3′), 4.25–4.40 (m, 1 H, H-4′), 3.95–4.15 (m, 2 H, H_2-5′), 0.85–1.15 (m, 28 H, 4 × Pr^i); FAB-MS *m*/*z* 684 [(M + H^+)], 572 [(M − OCOIm)$^+$], 469 [(M − B)$^+$], 357 [(M − B − OCOIm)$^+$]; R_f 0.77 (system A).

4-*N*-Benzoyl-3′,5′-*O*-(1,1,3,3-tetraisopropyldisiloxane-1,3-diyl)-2′-*O*-{[6-(trifluoroacetamido)hexyl]carbamoyl}cytidine 3. Imidazolide **2** (720 mg, 1.05 mmol) was stirred in 40 ml of dichloromethane with 445 mg of *N*-trifluoroacetyl-1,6-diaminohexane (2.1 mmol, 2 eq.) for 1.5 h. The latter was prepared by monoacylation of hexamethylenediamine with ethyl trifluoroacetate.[39] The reaction mixture was applied to a silica column and product was isolated using a gradient of methanol (0–3%) in dichloromethane. Fractions containing product were evaporated *in vacuo* to give a white solid foam (721 mg, 83%); ^{1}H NMR (DMSO-d_6) δ 11.47 [s, 1 H, NH (Cyt)], 9.52 (t, 1 H, $NHCOCF_3$, *J* 5.3 Hz), 8.27 (d, 1 H, H-6, $J_{6,5}$ 7.5 Hz), 8.12 (d, 2 H, Bz, *J* 7.1 Hz), 7.50–7.80 [m, 5 H, 3 H (Bz) + H-5 + NHCOO], 5.88 (s, 1 H, H-1′), 5.44 (d, 1 H, H-2′, *J* 5.1 Hz), 4.50–4.55 (m, 1 H, H-3′), 4.30–4.40 (m, 1 H, H-4′), 4.05–4.15 (m, 2 H, H_2-5′), 3.25–3.35 (m, 2 H, CH_2N), 2.95–3.20 (m, 2 H, CH_2N), 1.50–1.70 (m, 4 H, 2 × CH_2 internal), 1.30–1.50 (m, 4 H, 2 × CH_2 internal), 1.05–1.25 (m, 28 H, 4 × Pr^i); FAB-MS *m*/*z* 850 [(M + $Na)^+$], 828 [(M + $H)^+$], 613 [(M − B)$^+$], 357 [(M − B − OCONHalkyl)$^+$]; R_f 0.75 (system A).

4-*N*-Benzoyl-2′-*O*-{[(6-trifluoroacetamido)hexyl]carbamoyl}-cytidine 4. The 3′,5′-*O*-silyl-protected nucleoside derivative **3** (715 mg, 0.86 mmol) was dissolved in 5 ml of THF. A solution of TBAF (2.1 eq., 1.81 mmol, 474 mg) in 2 ml of THF was added and the slightly yellow solution was kept at room

temperature for 20 min. The product was precipitated by the addition of 50 ml of water. Precipitate was filtered off, and washed with water several times. Product was recrystallized from aq. ethanol to give 422 mg of a *white powder* (84%); ^{1}H NMR (DMSO-d_6) δ 11.42 [s, 1 H, NH (Cyt)], 9.51 (br t, 1 H, $NHCOCF_3$, J 5.0 Hz), 8.57 (d, 1 H, H-6, $J_{6,5}$ 7.5 Hz), 8.13 (d, 2 H, Bz, J 7.2 Hz), 7.60–7.85 (m, 3 H, Bz), 7.49 (d, 1 H, H-5), 7.43 (t, 1 H, NHCOO, J 5.6 Hz), 6.11 (d, 1 H, H-1′, $J_{1',2'}$ 4.0 Hz), 5.58 (d, 1 H, 3′-OH, J 5.3 Hz), 5.37 (m, 1 H, H-2′), 5.20 (t, 1 H, 5′-OH, J 4.6 Hz), 4.33 (m, 1 H, H-3′), 4.00–4.10 (m, 1 H, H-4′), 3.70–3.95 (m, 2 H, H_2-5′), 3.27 (m, 2 H, CH_2N), 3.07 (m, 2 H, CH_2N), 1.50–1.70 (m, 4 H, 2 × CH_2 internal), 1.30–1.45 (m, 4 H, 2 × CH_2 internal); FAB-MS *m*/*z* 608 [(M + Na)$^+$], 586 [(M + H)$^+$], 371 [(M − B)$^+$], 330 [(M − OCONHalkyl)$^+$], 216 (BH_2^+); R_f 0.34 (system A); mp 209–211 °C (Calc. for $C_{25}H_{30}F_3N_5O_8 \cdot H_2O$: C, 49.75; H, 5.35; N, 11.60. Found: C, 50.00; H, 5.02; N, 11.50%).

4-*N*-Benzoyl-5′-*O*-(4,4′-dimethoxytrityl)-2′-*O*-{[6-(trifluoroacetamido)hexyl]carbamoyl}cytidine 5. The 2′-modified nucleoside **4** (415 mg, 0.71 mmol) was evaporated with dry pyridine (2 × 10 ml), dissolved in 10 ml of the same solvent, and DMTrCl (1.25 eq., 0.88 mmol, 298 mg) was added. After 4 h at room temperature, the reaction mixture was poured into 5% aq. $NaHCO_3$ (50 ml), and extracted with dichloromethane (3 × 25 ml). Extract was washed successively with aq. $NaHCO_3$ (25 ml) and water (25 ml), dried over sodium sulfate, and evaporated *in vacuo*. Excess of pyridine was removed by coevaporation with toluene (2 × 10 ml). Product was isolated by silica gel column chromatography using a gradient of methanol (0–4%) in dichloromethane. Fractions containing tritylated product were evaporated *in vacuo* to give a slightly yellowish solid foam (528 mg, 84%); ^{1}H NMR (DMSO-d_6) δ 11.44 [s, 1 H, NH (Cyt)], 9.52 (br t, 1 H, $NHCOCF_3$, J 5.2 Hz), 8.43 (d, 1 H, H-6, $J_{6,5}$ 7.5 Hz), 8.12 (d, 2 H, Bz, J 7.1 Hz), 7.0–7.8 [m, 18 H, 3 H (Bz) + H-5 + NHCOO + 13 H (DMTr)], 6.06 (d, 1 H, H-1′, J 2.6 Hz), 5.68 (d, 1 H, 3′-OH, J 5.7 Hz), 5.30 (m, 1 H, H-2′), 4.55 (m, 1 H, H-3′), 4.15 (m, 1 H, H-4′), 3.87 (s, 6 H, 2 × OCH_3), 3.4–3.6 (H-5′, overlapping with water signal), 3.27 (m, 2 H, CH_2N), 3.09 (m, 2 H, CH_2N), 1.50–1.70 (m, 4 H, 2 × CH_2 internal), 1.30–1.45 (m, 4 H, 2 × CH_2 internal); FAB-MS *m*/*z* 910 [(M + Na)$^+$], 888 [(M + H)$^+$], 584 [(M − B)$^+$], 330 [(M − DMTr)$^+$], 303 ($DMTr^+$); R_f 0.69 (system A).

4-*N*-Benzoyl-5′-*O*-(4,4′-dimethoxytrityl)-2′-*O*-{[6-(trifluoroacetamido)hexyl]carbamoyl}cytidin-3′-yl 2-cyanoethyl *N*,*N*-diisopropylphosphoramidite 6. The 5′-O-tritylated nucleoside **5** (523 mg, 0.59 mmol) was evaporated twice with dry dichloromethane and dried under vacuum over P_2O_5 for 2 h. It was dissolved in 4 ml of dry CH_2Cl_2, and 4 eq. of DIPEA were added (2.36 mmol, 408 µl). The mixture, under N_2, was cooled (ice-bath) before the phosphitylating reagent, 2-cyanoethyl *N*,*N*-diisopropylchlorophosphoramidite (2 eq., 1.18 mmol, 263 µl), was added dropwise by syringe over a period of 5 min with stirring. The mixture was stirred for 10 min at ice-bath, then the bath was removed, and stirring was continued at room temperature. During 1.5 h, 200 µl of methanol was added. The mixture was diluted 10 min later with 25 ml of dichloromethane, washed successively with saturated aq. $NaHCO_3$ (2 × 15 ml) and saturated aq. NaCl (15 ml), dried over Na_2SO_4, and evaporated under vacuum. The residue was dissolved in $CHCl_3$–TEA (90 : 10) and applied to a silica column equilibrated with the same solvent. The column was washed with two volumes of this eluent, and then product was eluted with $CHCl_3$–EtOAc–TEA (45 : 45 : 10). Corresponding fractions were evaporated under vacuum. The amidite was precipitated from chloroform into hexane, filtered, washed with hexane, and dried under vacuum over phosphorus pentaoxide to give a white powder (474 mg, 74%). The product was stored in a refrigerator under nitrogen. Separation of diastereomers of phosphoramidite **6** by silica gel chromatography was possible; a 'fast' isomer was eluted with $CHCl_3$–EtOAc–TEA 7 : 2 : 1, whereas a 'slow' diastereomer eluted with the same system in the proportions 45 : 45 : 10. Purity of individual isomers was >90%, as was shown by ^{31}P NMR. (a) 'Fast' isomer: R_f 0.68 (system B); ^{1}H NMR (DMSO-d_6) δ 6.10 (d, 1 H, H-1′, J 4.1 Hz), 5.48 (m, 1 H, H-3′); ^{31}P NMR (DMSO-d_6) δ 150.2. (b) 'Slow' isomer: R_f 0.53 (system B); ^{1}H NMR (DMSO-d_6) δ 6.14 (d, 1 H, H-1′, J 4.6 Hz), 5.51 (m, 1 H, H-3′); ^{31}P NMR (DMSO-d_6) δ 149.6; FAB-MS of both isomers, *m*/*z* 1110 [(M + Na)$^+$], 1088 [(M + H)$^+$], 987 [(M − Pr^i_2N)$^+$], 683 [(M − Pr^i_2N − DMTr)$^+$], 566 {[(M − $Pr^i_2NP(OH)OCH_2CH_2CN$ − DMTr]$^+$}.

Oligonucleotides

The oligonucleotides (19- and 35-mer ODNs) were synthesized by solid-phase β-cyanoethyl phosphoramidite chemistry. The 35-mer ODN was purified by 20% polyacrylamide gel electrophoresis and desalted on a Sep-pak cartridge from Waters. The 19-mer ODNs containing a modified cytidine with an aminoalkyl linker at the C^5, C^6 or C^{11} position were obtained by direct incorporation of one cytidine amidite precursor **6** in the sequence of ODN. The coupling time for amidite reagent **6** (0.1 M in acetonitrile) was increased to 2 min. The HPLC analysis retention times of the 2′-O-aminoalkyl-modified ODNs were 38, 39 and 39 min for the C^5-, C^6- and C^{11}-modified ODNs, respectively. Detection was at 260 nm. The 2′-O-aminoalkyl-linker-modified ODNs were purified by HPLC under the same conditions as described for analysis and were desalted on Sep-pak cartridges before the coupling reaction with the metalloporphyrin entity. Concentrations of the ODNs were deduced from UV-absorbance measurements at 260 nm taking ε-values from the literature.[40]

Synthesis of manganese(III) tris(*N*-methylpyridinium-4-yl)-porphyrin–oligonucleotide conjugates

The manganese(III) 5-[(4-(carboxybutoxy)phenyl]-10,15,20-tris(*N*-methylpyridinium-4-yl)porphyrin precursor bearing a carboxylate group was prepared as described.[41] The metalloporphyrin–ODN conjugate at the 5′-end was prepared as described.[11] The coupling reaction between the purified C^5, C^6 and C^{11} 2′-*O*-aminoalkyl-modified ODNs and the metalloporphyrin involved the activation of a carboxylic function of a metalloporphyrin precursor by BOP and HOBT as a first step. The coupling reaction was performed according to the method of Duarte *et al.*[32] and was analyzed by HPLC using an anion-exchange column as described above. Detection of the products was at 260 and 468 nm simultaneously. The yield of the coupling reaction was around 90%. The impurities consisted of either unchanged starting 2′-*O*-aminoalkyl-modified ODN or one ODN product containing two metalloporphyrin moieties. The retention times were 27, 28 and 27 min for the C^5-, C^6- and C^{11}-modified conjugates, respectively. The conjugates were purified by HPLC using the same conditions as described for the analyses. Yields were approximatively 70% with respect to the starting 2′-*O*-aminoalkyl ODN (after purification and desalting of the conjugate); λ_{max} (H_2O) 262 and 468 nm, calculated ε_{260} = 190 000 M^{-1} cm^{-1} and ε_{468} = 130 000 M^{-1} cm^{-1}, observed visible–UV ratio on the diode array detector spectra of the conjugate HPLC peak was 0.7; ESI-MS (negative mode) *m*/*z* 951.5 [(M − 7H)$^{7-}$], 1110.0 [(M − 6H)$^{6-}$], 1332.0 [(M − 5H)$^{5-}$], 1665.5 [(M − 4H)$^{4-}$], 2221.0 [(M − 3H)$^{3-}$] compared to calculated 951.25, 1109.95, 1332.15, 1665.43 and 2220.9. The calculated neutral mass of the three metalloporphyrin–ODN conjugates was 4155.8 Da. Concentration of metalloporphyrin–ODN conjugate solutions was determined by UV absorbance at 260 nm as for single-stranded ODNs.

Cleavage of the 35-mer oligonucleotide

Labelling at the 5′-end of the 35-mer ODN was achieved by treatment with [γ-^{32}P]ATP from Amersham and T4 polynucleotide kinase from Gibco-BRL using the standard procedure. DNA-cleavage reactions (final reaction volume = 15 μl) were performed with 5′-[^{32}P]labelled 35-mer ODN target (final concentration 100 nM; 20×10^3 cpm) and the corresponding metalloporphyrin–ODN conjugates (final concentration 100 nM) in the presence of an excess of random double-stranded herring testes DNA (0.4 mM in nucleotides) in 100 mM NaCl, 50 mM phosphate buffer (pH 7). Annealing of the conjugates with complementary 35-mer was achieved by heating at 90 °C for 1 min followed by slow cooling to 25 °C. DNA-cleavage reactions were initiated by adding 1 μl of a freshly prepared solution of $KHSO_5$ (final concentration 0.01 or 0.1 mM). The DNA-cleavage reaction lasted 1 h at 0 °C and was stopped by the addition of 1 μl of 1 M HEPES buffer pH 8. The DNA material was precipitated overnight at −20 °C after addition of 100 μl of 0.3 M sodium acetate buffer (pH 5.2) containing 0.1 mg ml^{-1} yeast tRNA and 200 μl of cold ethanol. After centrifugation (10 min; 4 °C; 12×10^3 rpm), the DNA pellet was washed with cold 90% ethanol, dried under vacuum (Speedvac), dissolved in 100 μl of 1 M piperidine and incubated at 90 °C for 40 min. Samples were then evaporated to dryness, the DNA pellet was washed/dried twice with water to remove excess of piperidine, and dissolved in formamide with marker dyes. DNA fragments were analyzed by electrophoresis on denaturing (7 M urea) 20% polyacrylamide gel (3 h at 2300 V).

Acknowledgements

Igor Dubey is indebted to the Université Paul Sabatier (Toulouse) for financial support. Dr Henri-Louis Plaisancié from Isoprim (Toulouse) is acknowledged for the preparation of 2′-amino-linked ODNs. We are grateful to Dr Béatrice Mestre for providing a sample of the metalloporphyrin precursor.

References

1 J. Bernadou, G. Pratviel, F. Bennis, M. Girardet and B. Meunier, *Biochemistry*, 1989, **28**, 7268.
2 M. Pitié, J. Bernadou and B. Meunier, *J. Am. Chem. Soc.*, 1995, **117**, 2935.
3 J. Bernadou and B. Meunier, *Chem. Commun.*, 1998, 2167.
4 J. T. Groves, J. Lee and S. S. Marla, *J. Am. Chem. Soc.*, 1997, **119**, 6269.
5 M. Pitié, G. Pratviel, J. Bernadou and B. Meunier, *Proc. Natl. Acad. Sci. U.S.A.*, 1992, **89**, 3967.
6 C. Vialas, G. Pratviel, C. Claparols and B. Meunier, *J. Am. Chem. Soc.*, 1998, **120**, 11548.
7 C. Vialas, C. Claparols, G. Pratviel and B. Meunier, *J. Am. Chem. Soc.*, 2000, **122**, 2157.
8 G. Pratviel, V. Duarte, J. Bernadou and B. Meunier, *J. Am. Chem. Soc.*, 1993, **115**, 7939.
9 M. Pitié, C. Casas, C. J. Lacey, G. Pratviel, J. Bernadou and B. Meunier, *Angew. Chem., Int. Ed. Engl.*, 1993, **32**, 557.
10 B. Mestre, G. Pratviel and B. Meunier, *Bioconjugate Chem.*, 1995, **6**, 466.
11 B. Mestre, A. Jacobs, G. Pratviel and B. Meunier, *Biochemistry*, 1996, **35**, 9140.
12 P. Bigey, G. Pratviel and B. Meunier, *Nucleic Acids Res.*, 1995, **23**, 3894.
13 B. Mestre, M. Pitié, C. Loup, C. Claparols, G. Pratviel and B. Meunier, *Nucleic Acids Res.*, 1997, **25**, 1022.
14 G. Pratviel, J. Bernadou and B. Meunier, *Angew. Chem., Int. Ed. Engl.*, 1995, **34**, 746.
15 G. Pratviel, J. Bernadou and B. Meunier, *Adv. Inorg. Chem.*, 1998, **45**, 251.
16 L. C. Griffin, L. L. Kiessling, P. A. Beal, P. Gillespie and P. B. Dervan, *J. Am. Chem. Soc.*, 1992, **114**, 7976.
17 D. S. Sigman, T. W. Bruice, A. Mazumder and C. L. Sutton, *Acc. Chem. Res.*, 1993, **26**, 98.
18 J. T. Groves and I. O. Kady, *Inorg. Chem.*, 1993, **32**, 3868.
19 D. E. Bergstrom and N. P. Gerry, *J. Am. Chem. Soc.*, 1994, **116**, 12067.
20 H. Inoue, Y. Hayase, A. Imura, S. Iwai, K. Miura and E. Ohtsuka, *Nucleic Acids Res.*, 1987, **15**, 6131.
21 A. M. Iribarren, B. S. Sproat, P. Neuner, I. Sulston, U. Ryder and A. I. Lamond, *Proc. Natl. Acad. Sci. U.S.A.*, 1990, **87**, 7747.
22 B. S. Sproat and A. I. Lamond, in *Antisense Research and Applications*, ed. S. T. Crooke and B. Lebleu, CRC Press, Boca Raton, FL, 1993, pp. 351–362.
23 K. Yamana, Y. Nishijima, T. Ikeda, T. Gokota, H. Ozaki, H. Nakano, O. Sangen and T. Shimidzu, *Bioconjugate Chem.*, 1990, **1**, 319.
24 H. M. Desmukh, S. P. Joglekar and A. D. Broom, *Bioconjugate Chem.*, 1995, **6**, 578.
25 K. Yamana, R. Aota and H. Nakano, *Tetrahedron Lett.*, 1995, **36**, 8427.
26 K. Yamana, Y. Ohashi, K. Nunota, M. Kitamura, H. Nakano, O. Sangen and T. Shimidzu, *Tetrahedron Lett.*, 1991, **32**, 6347.
27 K. Yamana, Y. Ohashi, K. Nunota and H. Nakano, *Tetrahedron*, 1997, **53**, 4265.
28 M. Manoharan, C. J. Guinosso and P. D. Cook, *Tetrahedron Lett.*, 1991, **32**, 7171.
29 M. Manoharan, L. K. Johnson, K. L. Tivel, R. H. Springer and P. D. Cook, *Bioorg. Med. Chem. Lett.*, 1993, **3**, 2765.
30 E. A. Lesnik, C. J. Guinosso, A. M. Kawasaki, H. Sasmor, M. Zounes, L. L. Cummins, D. J. Ecker, P. D. Cook and S. M. Freier, *Biochemistry*, 1993, **32**, 7832.
31 M. E. Douglas, B. Beijer and B. S. Sproat, *Bioorg. Med. Chem. Lett.*, 1994, **4**, 995.
32 V. Duarte, G. Pratviel, B. Meunier, M. Berton, S. Sixou and G. Favre, *New J. Chem.*, 1997, **21**, 55.
33 H. Sugiyama and I. Saito, *J. Am. Chem. Soc.*, 1996, **118**, 7063.
34 K. E. Erkkila, D. T. Odom and J. K. Barton, *Chem. Rev.*, 1999, **99**, 2777.
35 B. Giese, S. Wessely, M. Spormann, U. Lindemann, E. Meggers and M. E. Michel-Beyerle, *Angew. Chem., Int. Ed.*, 1999, **38**, 996.
36 Y. Kan and G. B. Schuster, *J. Am. Chem. Soc.*, 1999, **121**, 10857.
37 K. A. Watanabe and J. J. Fox, *Angew. Chem., Int. Ed. Engl.*, 1966, **5**, 589.
38 B. S. Sproat and A. I. Lamond, in *Oligonucleotides and Analogues: a Practical Approach, the Practical Approach Series*, ed. F. Eckstein, Oxford University Press, Oxford, New York, Tokyo, 1991, pp. 49–86.
39 S. Agrawal and J.-Y. Tang, *Tetrahedron Lett.*, 1990, **31**, 1543.
40 *Handbook of Biochemistry and Molecular Biology – Nucleic Acids*, ed. G. Fasman, CRC Press, Cleveland, 3rd edn., 1975, p. 175.
41 C. Casas, B. Saint-Jalmes, C. Loup, C. J. Lacey and B. Meunier, *J. Org. Chem.*, 1993, **58**, 2913.